An Improved Finite Difference Method for Fixed-Bed Multicomponent Sorption

L. M. Sun and F. Meunier
LIMSI-CNRS, BP.133 91403 Orsay, France

A new computational procedure based on the finite difference methods is developed to solve the coupled partial differential equations describing nonisothermal and nonequilibrium sorption of multiple adsorbate systems on a fixed bed that contains bidispersed pellets. In this numerical method, a solution-adaptive gridding technique (SAG) is applied in combination with a four-point quadratic upstream differencing scheme to satisfactorily resolve very sharp concentration and temperature variations occurring in the case of small dispersing effects. Furthermore, the method resorts to a noniterative implicit procedure for solving the coupling between the column transport equations and the adsorption kinetics inside the pellets, which may be particularly efficient when the particle kinetics equations are highly stiff.

The numerical model will be tested for one-, two- and three-transition systems. The results are compared to available analytical and equilibrium theory solutions.

Introduction

Adsorption processes are utilized widely in chemical and petrochemical industries and are becoming increasingly attractive in biotechnology and environmental control engineering. For an optimal design of an industrial adsorptive process, it is important to have accurate modeling and simulation of the dynamic behavior of fixed-bed adsorbers.

A complete mathematical model describing the sorption of a multicomponent adsorbate system on fixed beds has to take into account the following mechanisms:

- Heat and mass transports of the mixture outside the solid phase, which are generally characterized by convection-diffusion equations
- Heat conduction and mass diffusion inside the adsorbent particles, which may contain two scales: the pellet scale and the crystallite scale as in the case of zeolite pellets.
- Adsorption isotherms, diffusion and surface transfer coefficients, and other physical properties as functions of partial pressures and temperatures.

The complexity and nonlinearity of such models in general exclude the possibility of having an analytical solution. Even in linear and extremely simplified cases, analytical solutions are scarce and generally slowly converging (Raghavan and Ruthven, 1983). Therefore, numerical methods are the only feasible alternative to meet the requirements for the simulation of fixed-bed dynamics. These requirements can be an accurate resolution of convection-diffusion equations, ability to solve the coupling between the different components which may be described either by simple adsorption isotherms or by complicated differential equations. Further, with numerical models it would be possible to account for the nonlinearity due to the adsorption isotherms and physical properties, as well as the possibility of straightforward extension to cyclic processes with varying boundary and initial conditions.

Considerable advances have been made in recent years in numerical simulations of the multicomponent adsorption. A number of sophisticated models have been successfully developed generally by implementing finite difference methods, the method of characteristics and the method of orthogonal collocation. The finite difference methods are frequently utilized due to their simplicity, efficiency in solving parabolic equations, and ease of varying initial and boundary conditions (Carter and Husain, 1974; Cooney, 1974; Chihara and Suzuki, 1983; Doong and Yang, 1986; Huang and Fair, 1988). It should be noted that two major difficulties may be encountered in the simulation of fixed-bed dynamics using finite differences. These are the resolution of convection-diffusion equations and modeling of the coupling between adsorbate components. The first difficulty arises with highly convective problems and is worsened by the self-sharpening effect of favorable adsorption isotherms. The use of traditional first-order upstream differ-

encing yields important false diffusion, while central differencing presents large unphysical oscillations. Such undesirable behaviors can be eliminated or reduced by increasing the number of computational grids, but this approach often proves to be unrealistic and expensive. The second obstacle comes from the solution of coupled differential equations: use of explicit schemes avoids matrix inversions but suffers generally from severe stability limitations. Implicit schemes are more accurate and unconditionally stable but require the inversion of generally large matrices.

Most of the previous works using finite difference methods in fixed-bed dynamics applied either first-order upstream or second-order central difference approximations with uniform grid spacing. In the solution procedure of the coupled discretized equations, either explicit schemes or iterative implicit schemes have been used. For the implicit formulation, the column and particle equations are decoupled at each iteration level. As a consequence, these methods proved to be unsatisfactory for highly convective flows or very time-consuming due to small time step requirements imposed by the convergence considerations, in particular when the particle kinetics equations are stiff. Further efforts are, therefore, necessary for development of solution procedures for convection-diffusion equations as well as modeling of the coupling at the column-pellet and pellet-crystallite interfaces. It is essential that these solution procedures are robust and computationally cost-effective.

Numerical difficulties with the finite difference approximations for the solution of convection-diffusion equations have been studied extensively in the computational fluid dynamics field. A number of improved methods have been successfully applied to simulations of sharp front problems. These methods are essentially based on two different grid discretizations: fixed grids (Sod, 1978; Patel et al., 1985) and adaptive gridding techniques (Thompson, 1984). The former methods try to reduce oscillatory behaviors of high-order differencing schemes and the latter concentrate the grids around large gradient regions in an optimum manner. Certainly, both techniques can be associated with numerical simulations of related problems, and the combination of both proved feasible (Hu and Schiesser, 1981).

These numerical tools can also be applied to simulations of multicomponent adsorption systems. However, except for the contributions of Schiesser and coworkers (Hu et al., 1982) who used an adaptive grid for a separation system, no application of these techniques can be found in the literature.

In this study, the application of the adaptive gridding method is extended to the problems of multicomponent adsorption systems. Special attention is paid to the treatment of thermal effects as well as particle kinetics.

The theoretical model presented describes a nonisothermal and nonequilibrium flow through a column that is composed of biporous adsorbent particles. The equations are then approximated by finite differences using an adaptive gridding technique and an implicit solution procedure. Results are first obtained in the equilibrium case, which subsequently are compared with analytical or equilibrium theory solutions. Then, effects of adsorption kinetics are presented.

Mathematical Model

Fixed-bed dynamics are described basically by a set of convection-diffusion equations, coupled with source terms due to adsorption and diffusion inside adsorbent particles. Mathematical modeling of this kind of problems has been largely studied, and excellent reviews can be found in the literature (e.g., Ruthven, 1984; Yang, 1987). The system considered here is a column composed of biporous adsorbent particles (as in the case of zeolite pellets), which is subjected to a constant feed at the inlet. The following assumptions have been made in the development of a general model in the case of dilute systems:

1. The flow velocity is constant.
2. Radial effects are neglected.
3. Gaseous components behave as ideal gases.
4. Temperature is uniform inside the adsorbent particles.
5. The crossed terms in the driving force for mass diffusion are neglected and the driving force for the microporous diffusion in the crystallites is proportional to the gradient of adsorbate chemical potentials, i.e.,

$$J = -Bq\nabla\mu = -B_c\nabla p \qquad (B_c = BqRT_s/p) \tag{1}$$

The modified mobility B_c is related to the traditional diffusion coefficient D_i by $D_i = B_c(\partial p/\partial q)_{T_s}$. The macroporous diffusion is supposed to be essentially in the Knudsen regime and the simple Fick's law can be used.

6. All the transfer coefficients are constant.
7. Pellets and crystallites are considered as spherical particles and uniformly distributed.
8. The equilibrium between the gas phase in the macropores and the adsorbate phase in the micropores is maintained at the crystallites' surface. This assumption is reasonable since the surface barrier effect is generally included in the effective microporous diffusion coefficient.

Under the above assumptions, the governing equations and appropriate initial and boundary equations can be written as follows:

Mass and energy balances for the gas phase in the bed void:

$$\frac{\partial c_k}{\partial t} + \frac{\partial (uc_k)}{\partial z} - \frac{\partial}{\partial z}\left(D_k \frac{\partial c_k}{\partial z}\right) + \frac{1-\epsilon_b}{\epsilon_b}\left[\epsilon_p \frac{\partial \bar{c}_{pk}}{\partial t} + (1-\epsilon_p)\frac{\partial \bar{\bar{q}}_k}{\partial t}\right] = 0 \tag{2}$$

$$C_M \frac{\partial T_f}{\partial t} + \frac{\partial (uC_M T_f)}{\partial z} - \frac{\partial}{\partial z}\left(\lambda_M \frac{\partial T_f}{\partial z}\right) = \frac{2h_w}{\epsilon_b R_b}(T_w - T_f) + \frac{1-\epsilon_b}{\epsilon_b}\frac{3h}{R_p}(T_s - T_f) \tag{3}$$

where $\bar{\bar{q}}$ represents the adsorbed quantity q averaged first over a crystallite volume and then over a pellet volume.

Initial and boundary conditions:

$$t<0: \quad c_k = c_{0,k}; \quad T_f = T_0 \text{ for } 0 \le z \le L_b$$

$$z=0: \quad c_k = c_{in,k}; \quad T_f = T_{in} \text{ for } t \ge 0$$

$$z=L_b: \quad \frac{\partial c_k}{\partial z} = 0; \quad \frac{\partial T_f}{\partial z} = 0 \text{ for } t \ge 0$$

Macroporous diffusion at the pellet scale:

$$\frac{\partial c_{pk}}{\partial t}+\frac{1-\epsilon_p}{\epsilon_p}\frac{\partial \bar{q}_k}{\partial t}=\frac{1}{r_p^2}\frac{\partial}{\partial r_p}\left(D_{pk}r_p^2\frac{\partial c_{pk}}{\partial r_p}\right) \tag{4}$$

$$\left.\frac{\partial c_{pk}}{\partial r_p}\right|_{r_p=0}=0 \tag{5}$$

$$-D_{pk}\left.\frac{\partial c_{pk}}{\partial r_p}\right|_{r_p=R_p}=k_{pk}(c_{pk}|_{r_p=R_p}-c_k) \tag{6}$$

where $\bar{q}$ represents q averaged only over a crystallite volume.

Overall heat balance on the pellet:

$$C_s\frac{\partial T_s}{\partial t}-(1-\epsilon_p)\sum_{k=1}^{m}(-\Delta H_k)\frac{\partial \bar{\bar{q}}_k}{\partial t}=\frac{3h_p}{R_p}(T_f-T_s) \tag{7}$$

Microporous diffusion at the crystallite scale:

$$\frac{\partial q_k}{\partial t}=\frac{1}{r_i^2}\frac{\partial}{\partial r_i}\left(B_{ck}\,r_i^2\frac{\partial p_k}{\partial r_i}\right) \tag{8}$$

$$\left.\frac{\partial p_k}{\partial r_i}\right|_{r_i=0}=0 \tag{9}$$

$$p_k|_{r_i=R_i}=c_{pk}R_kT_s=\phi_k\,c_{pk} \tag{10}$$

The above equations are to be coupled with mixture adsorption isotherms which give the relationship between the adsorbed concentrations q, the temperature T_s, and the partial pressures p. To avoid complicated nonlinear boundary conditions, we take the partial pressures as dependent variables at the crystallite scale, rather than the commonly used adsorbate concentrations. In this way, Eq. 10 can be treated as a linear relation but with a variable coefficient $\phi=RT_s$.

The two-scale description of adsorption kinetics within the pellets in the PDE form is very cumbersome for numerical calculations. Therefore, the well-known parabolic profile approach will be applied here. This simplifying approach has been used with success in many cases (Yang, 1987). With this simplification and a partial normalization, Eqs. 2-10 can be rewritten as:

$$\frac{\partial c_k}{\partial \tau}+\frac{\partial c_k}{\partial x}-\frac{1}{Pe_k}\frac{\partial^2 c_k}{\partial x^2}+E\left(\frac{\partial \bar{c}_{pk}}{\partial \tau}+F\sum_{j=1}^{m+1}Q_{kj}\frac{\partial \omega_j}{\partial \tau}\right)=0 \tag{11}$$

$$\frac{\partial T_f}{\partial \tau}+\frac{\partial T_f}{\partial x}-\frac{1}{Pe_{m+1}}\frac{\partial^2 T_f}{\partial x^2}=\alpha_W(T_w-T_f)+UV\sum_{j=1}^{m+1}Z_j\frac{\partial \omega_j}{\partial \tau}-U\frac{\partial \omega_{m+1}}{\partial \tau} \tag{12}$$

$$\frac{\partial \bar{c}_{pk}}{\partial \tau}+F\sum_{j=1}^{m+1}Q_{kj}\frac{\partial \omega_j}{\partial \tau}=\alpha_{Pk}(c_k-\bar{c}_{pk}) \tag{13}$$

$$\sum_{j=1}^{m+1}Q_{kj}\frac{\partial \omega_j}{\partial \tau}=\alpha_{Ik}Q_k^*(\phi_k\bar{c}_{pk}-\omega_k) \tag{14}$$

$$\frac{\partial \omega_{m+1}}{\partial \tau}=\alpha_H(T_f-\omega_{m+1})+V\sum_{j=1}^{m+1}Z_j\frac{\partial \omega}{\partial \tau} \tag{15}$$

where $\omega_j=\bar{\bar{p}}_j$ for $j\le m$ and $\omega_{m+1}=T_s$, Q and Z depend only on derivatives of the adsorption isotherm and on the heat of adsorption:

$$Q_{kj}=\frac{\partial \bar{\bar{q}}_k}{\partial \omega_j}\quad Z_j=\sum_{k=1}^{m}(-\Delta H_k)Q_{kj} \tag{16}$$

Q_k^* is obtained by calculating Q_{kk} at a reference state and was introduced to have a traditional diffusion coefficient $D_{ik}=B_{ck}/Q_k^*$. Other constant parameters are defined by:

$$E=\frac{1-\epsilon_b}{\epsilon_b}\epsilon_p\quad F=\frac{1-\epsilon_p}{\epsilon_p}\quad U=\frac{(1-\epsilon_b)C_S}{\epsilon_b C_M}\quad V=\frac{1-\epsilon_p}{C_s} \tag{17}$$

and

$$\alpha_H=\frac{3h_pL_b}{R_pC_S\,u}=\frac{\text{retention time of carrier gas}}{\text{time constant for heat exchange through pellets}} \tag{18}$$

$$\alpha_{Ik}=\frac{15D_{ik}L_b}{R_i^2\,u}=\frac{\text{retention time of carrier gas}}{\text{time constant for microporous diffusion}} \tag{19}$$

$$\alpha_{Pk}=\frac{15k_{pk}L_b}{R_pu(5+k_{pk}R_p/D_{pk})}=\frac{\text{retention time of carrier gas}}{\text{time constant for macroporous diffusion}} \tag{20}$$

$$\alpha_W=\frac{2h_wL_b}{\epsilon_bR_bC_Mu}=\frac{\text{retention time of carrier gas}}{\text{time constant for heat exchange through wall}} \tag{21}$$

Equations 11-15 represent a set of $3m+2$ coupled quasilinear differential equations with the same number of unknown variables: m gas concentrations in the bed void c_k, m macroporous concentrations c_{pk}, m partial pressures p_k, and two temperatures T_f and T_s. The coupling between the variables is defined by ordinary differential equations through the adsorption isotherm and transfer coefficients.

Method of Solution

The differential equations (Eqs. 11-15) are parabolic and can be solved by a finite difference technique. Numerical solution of this system proves to be difficult due to the convective terms on the one hand and the coupling between the individual components on the other. The numerical method used is based on an explicit adaptive gridding technique with a four-point

quadratic upstream differencing for first-order derivatives and a noniterative solution procedure.

Grid structure

For one-dimensional highly convective flows, the adaptive gridding techniques have proven to be more feasible than the refining grid approach. Such techniques distribute optimally computational grids around sharp transitions and are in principle capable of capturing steep variations. The main shortcoming is that the differencing schemes become less accurate because of the use of nonuniform grids (Hoffman, 1982).

Two different approaches are available and can be qualified as implicit and explicit grid selection methods. In the implicit approach, grid selection and PDE solution are closely coupled and solution of a supplementary equation is necessary (White, 1982). In the explicit approach, the grid adaptation is based on the solutions obtained at the previous time level (Dwyer, 1984; Sanz-Serna and Christie, 1986; Blom et al., 1988). The implicit methods can endure very steep transitions. But with these methods, the original equations are complicated considerably and even likely to be ill-conditioned. On the other hand, the explicit methods cannot be expected to be successful with very sharp transitions and further require an interpolation step. The explicit solution adaptive gridding (SAG) techniques possess two very attractive features: simplicity and independence on the solution procedure. In the light of the above considerations, a SAG technique has been implemented in this study. This is essentially a modified version of the explicit regridding technique proposed by Sanz-Serna and Christie (1986).

In their original technique, all grids are changed to have approximately a piecewise constant arclength function. Consequently, the interpolation calculation needs to be performed for each grid at the regridding step. Herein, we adopt a different strategy and only a part of grids is changed. The computational grids are divided into two parts: *fixed* grids and *moving* grids. The fixed grids are used to avoid a large disparity in grid sizes and the moving grids to follow sharp transitions. The algorithm used is as follows:

Define first a cell arclength function to measure the sharpness of concentration and temperature fronts:

$$S_i=\Delta x_i\sum_{k=1}^{m+1}\left[1+a_1\left(\frac{\partial C_k}{\partial x}\right)_i^2+a_2\left(\frac{\partial^2 C_k}{\partial x^2}\right)_i^2\right]^{1/2}\quad\text{for } i=1,2,\ldots,N \tag{22}$$

where a_1 and a_2 are two arbitrarily-chosen constants and C_k represents normalized c_k ($k\le m$) and T_f ($k=m+1$). The normalization is made to have a uniform weighting between different components. This function will be used as a criterion for the regridding.

Knowing the solutions at a certain time step, we calculate S_i for each cell and the corresponding arithmetic mean $\bar{S}$. Then the moving grids will be redistributed according to the values of $S_i/\bar{S}$: a number of grids will be inserted in the cell i if $S_i/\bar{S}$ exceeds a certain value, and the moving grid i will be deleted if its $S_i/\bar{S}$ becomes small. The number of grids to be inserted is not only proportional to the value $S_i/\bar{S}$ but also to the number of available moving grids. Moreover, the grid insertion is made uniformly in the cells and the grids are uniform piecewise.

After that, a projection is performed from the old grids to the new grids by using cubic and quadratic interpolations for internal and boundary points, respectively. Obviously, the interpolation is necessary only for newly inserted grids.

As in the work of Sanz-Serna and Christie, we introduce a predefined limiting value S_{lim} for the cell arclength function S_i to avoid, in combination with the use of fixed grids, a disproportionate local distribution of grids.

Finite difference approximations

Since explicit schemes may suffer from severe stability limits, the implicit Crank-Nicolson scheme is used in the present work. This second-order scheme is chosen due to its two-level feature in spite of the fact that it may exhibit slightly worse properties of dampening small wavelength harmonics than some other schemes such as the three-level Richtmyer-Morton scheme (Peyret and Taylor, 1983). For spatial derivatives, diffusion terms are replaced by the central differencing which has a third-order consistency. Inaccuracies are due mainly to the difference approximation of first-order spatial derivatives. It is well-known that the first order upstream differencing scheme (UDS) yields substantial numerical diffusion and the second-order central differencing scheme (CDS) presents large oscillations (Peyret and Taylor, 1983). Therefore, in this work, a third-order quadratic upstream differencing scheme (QUDS) proposed by Leonard (Leonard, 1979) has been used. This is an excellent compromise between precision requirements and calculation costs (Patel et al., 1985).

The difference approximation of the spatial first-order derivative at grid i is given by:

$$\left(\frac{\partial c}{\partial x}\right)_i=\frac{c_{w,i}-c_{w,i-1}}{\Delta x_i} \tag{23}$$

where i is the grid subscript which increases in the flow direction. The cell wall point $c_{w,i}$ can be determined by an interpolation between neighboring cell points: for UDS, a zeroth-order interpolation is used with one single upstream point; for CDS, the cell wall points are evaluated by a linear interpolation between one upstream point and one downstream point and for QUDS, a quadratic interpolation is used with two upstream points and one downstream point. Namely,

$$c_{w,i}=\alpha_i\, c_{i-1}+\beta_i\, c_i+\gamma_i c_{i+1} \tag{24}$$

The values of α, β and γ are given in Table 1 for the above three schemes on nonuniform grids.

Both UDS and QUDS are biased toward the upstream direction and their numerical properties for large Peclet numbers are expected to be better than CDS. A Taylor series expansion shows that on uniform grids, UDS is accurate only for the first-order in Δx with a strong second-order dissipative term yielding large numerical diffusion (quantified by $u\Delta x/2$), CDS is accurate for the second-order with a third-order dispersive term leading to large numerical oscillation and QUDS is third-order-accurate with a fourth-order dissipative term which may dampen the fifth-order dispersive term.

In the case of a single equation, the three-point UDS and

Table 1. Definitions of α, β and γ on Nonuniform Grids

	UDS	CDS	QUDS
α_i	0	0	$-\Delta x_{i+1}^2/[4\Delta x_i(\Delta x_i+\Delta x_{i+1})]$
β_i	1	0.5	$0.5(1+0.5\Delta x_{i+1}/\Delta x_i)$
γ_i	0	0.5	$0.5[1-0.5\Delta x_{i+1}/(\Delta x_i+\Delta x_{i+1})]$

CDS yield a tridiagonal system while the four-point QUDS leads to a quadrdiagonal system. Therefore, calculation costs are not expected to considerably increase when QUDS is used.

Solution of PDEs on fixed grids

Replacing all the derivatives by their difference representations and approximating the boundary conditions by consistent extrapolations, a set of $(3m+2)\times N$ algebraic equations is obtained. The procedure for solving this system detailed in the Appendix primarily as follows. Since the column variables (c_k, T_f) and the particle variables (c_{pk}, p_k, T_s) are coupled through ordinary differential equations, we can first express the particle variables as functions of the column variables and then introduce these expressions into the column equations (Eqs. 11 and 12) to obtain a set of equations with only c_k and T_f as unknowns. This set of $(m+1)\times N$ column equations can be easily solved by an iterative method, in which only a single equation is solved at each step with the coupling terms evaluated by the most recent values. The iteration stops if a prescribed tolerance is satisfied. Once c_k and T_f are known, a back substitution is made to calculate the values of c_{pk}, p_k, and T_s.

Because of the nonlinear feature of the system, the above solution procedure needs to be iterated until a small difference between two iterations is reached. In the following calculations, a limiting value of 10^{-6} will be used for the L_1 norm of the relative difference vector.

Numerical Studies

As the standard case for numerical investigations, we consider sorption of the binary mixture CO_2 and C_2H_6 on beds of Linde 5A molecular sieves. The corresponding adsorption isotherm can be defined by a Langmuir-type relation (Liapis and Crosser, 1982):

$$q_k=\frac{q_{sk}b_kp_k}{1+\Sigma_j\, b_jp_j} \qquad (k,j=CO_2,\ C_2H_6)$$

$$\text{with } b_k=\frac{b_{0k}}{\sqrt{T}}\exp\left(-\frac{\Delta H_k}{R_kT}\right) \qquad (25)$$

where

$q_s=154.7\ kg/m^3$

$b_0=0.420\ 10^{-9}\ \text{Pa}^{-1}$

$\Delta H=-1.045\ 10^6\ J/kg$ for CO_2

$q_s=122.0\ kg/m^3$

$b_0=8.108\ 10^{-9}\ \text{Pa}^{-1}$

$\Delta H=-0.989\ 10^6\ J/kg$ for C_2H_6

Table 2. Parameter Values Used in the Simulations ($1\rightarrow CO_2$, $2\rightarrow C_2H_6$)

$u=0.20$ m/s	$\epsilon_b=0.38$	$\epsilon_p=0.52$
$L_b=0.5$ m	$R_b=0.03$ m	$R_p=0.001$ m
$T_0=24°C$	$T_w=24°C$	$h_w=0.0$ W/m^2/K
$h_p=100$ W/m^2/K	$C_M=1{,}435$ J/m^3/K	$C_s=1.028\ 10^6$ J/m^3/K
$D_1=2\ 10^{-4}$ m^2/s	$D_2=210^{-4}$ m^2/s	$\lambda_M/C_M=2\ 10^{-4}$ m^2/s
$k_{p1}=\infty$ m/s	$k_{p2}=\infty$ m/s	$D_{p1}=10^{-5}$ m^2/s
$D_{p2}=10^{-5}$ m^2/s	$D_{i1}=10^{-14}$ m^2/s	$D_{i2}=10^{-17}$ m^2/s
$a_1=0.0$	$a_2=1.0$	$S_{lim}=10^4$

The values of other physical and geometrical parameters are given in Table 2. These values yield the following constants used in Eqs. 11-15: $E=5.221\ 10^{-1}$, $F=2.125$, $U=1.169\ 10^3$, $V=6.615\ 10^{-7}$, $Pe_k=500$ $(k=1,2,3)$ and $\alpha_{I1}=2.919\ 10^{-1}$, $\alpha_{I1}=0.375$, $\alpha_{I2}=3.75\ 10^{-4}$, $\alpha_{P1}=375$, $\alpha_{P2}=375$, and $\alpha_W=0$.

Note from Table 2 that the limiting value for the arclength function used in this work is much larger than that of Sanz-Serna and Christie ($S_{lim}=10^2$). Nevertheless, this value has been proven to be reasonable due to the use of fixed grids. Another important numerical parameter is the ratio of the numbers of fixed and moving grids: approximately a third of the computational grids are utilized as fixed grids and the others as moving ones. The corresponding optimal choice will not be investigated.

In what follows, we will give systematically comparisons of the present numerical method (SAG) with uniform QUDS, CDS, and UDS methods. Numerical tests will be performed in several physical situations, in particular in the case of equilibrium plug flows where either analytical or equilibrium theory solutions may be available. Also we define the following errors to have quantitative comparisons:

$$\|e\|_\infty=\max_{k,i}\left|\frac{c_{k,i}-c_{k,i}^{(\text{exact})}}{c_{in,k}-c_{0,k}}\right|$$

$$\|e\|_2=\left[\sum_{i=1}^{N}\frac{\Delta x_i}{m+1}\sum_{k=1}^{m+1}\left(\frac{c_{k,i}-c_{k,i}^{(\text{exact})}}{c_{in,k}-c_{0,k}}\right)^2\right]^{1/2} \qquad (26)$$

where $c^{(\text{exact})}$ represent either analytical solutions or precise numerical solutions obtained by the use of more grids and of smaller time steps. In the latter case, the exact solutions can be considered only as a reference.

Comparison with equilibrium models

For sorption of a single adsorbate system under isothermal and equilibrium conditions, the analytical solution can be easily obtained if a linear adsorption isotherm and an infinite bed length are assumed (Ruthven, 1984). This difference in the outlet boundary condition between the analytical and numerical models does not lead to any perceptible discrepancy for large Peclet numbers. A typical comparison between analytical and numerical solutions is shown in Figure 1 for a highly convective flow ($Pe=5\ 10^4$) of CO_2. For numerical simulations, a deliberately large grid Peclet number is used: $Pe_\Delta=500$. As expected, UDS produces enormous false diffusion (250 times as large as the true dispersion) and CDS yields large unphysical oscillations. QUDS offers a very good compromise and dampens oscillations more rapidly. The present method (SAG) very

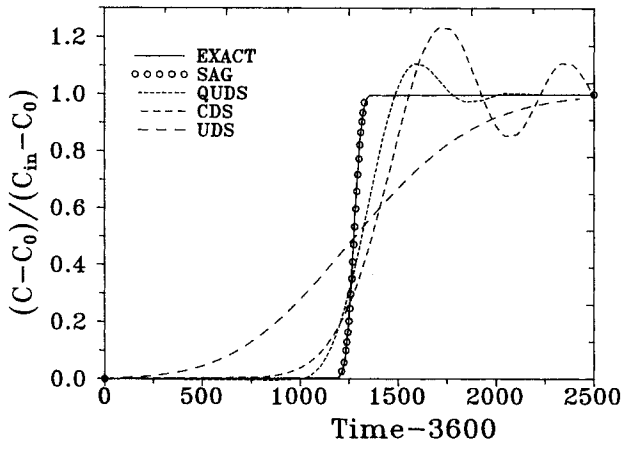

Figure 1. Breakthrough curves for a single transition system ($Pe = 5\ 10^4$). $Pe_\Delta = 500$ for the numerical simulations.

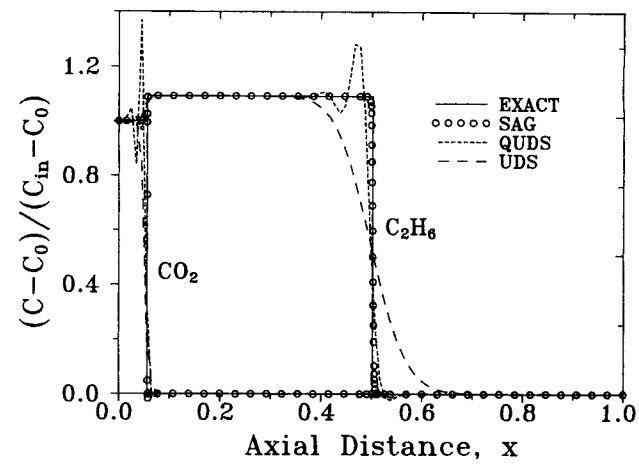

Figure 2. Profiles at $\tau = 2{,}000$ for isothermal adsorption of a binary mixture.

$Pe_\Delta = 100$ for finite difference models and "exact" solutions were obtained by use of the equilibrium theory. $(\|e\|_2, \|e\|_\infty) = (0.0042, 0.2132)$ for SAG, (0.0641, 0.6052) for QUDS and (0.0944, 0.7168) for UDS.

well describes the sharp concentration front ar d numerical oscillations are essentially eliminated. The erro s of the numerical models at $\tau = 3{,}000$ are given in Table 3 in terms of the grid Peclet number. This table confirms the superiority of the SAG technique over the uniform schemes and indicates a faster convergence for SAG. It is worthwhile to note that SAG does not increase the calculation cost considerably due to its explicit feature. The computer time consumed by the regridding and interpolation steps represents only a fraction of the total calculation time (inferior to 0.3).

There exist two or three distinct fronts in the case of a binary adsorbate system under equilibrium, isothermal or adiabatic conditions. The corresponding exact solutions can be obtained under the plug-flow condition by applying the equilibrium theory (Rhee and Amundson, 1970; Rhee et al., 1970). In this case, the governing equations are reduced to:

$$(1+E)\frac{\partial c_k}{\partial \tau} + \frac{\partial c_k}{\partial x} + EF\frac{\partial q_k}{\partial \tau} = 0 \quad \text{for } k = 1,2 \qquad (27)$$

In the case of a single adsorbate system under the adiabatic condition, c_2 and q_2 are redefined by:

$$c_2 = T_f \quad \text{and} \quad q_2 = \left(\frac{U-E}{EF}\right) T_f - \frac{(-\Delta H_1)}{C_M} q_1$$

For numerical models, related transfer coefficients are set to be infinite ($\alpha_H = \alpha_I = \alpha_P = \infty$) and a relatively large Peclet number is used ($Pe = 10^4$). Two situations are investigated:

1. *Saturation of a Clean Bed by the Binary Mixture under Isothermal Condition.* The partial pressures are $p_{0,k} = 10^{-5}$ and $p_{in,k} = 10^3$ (Pa) ($k = 1,2$). If a plug flow is assumed ($Pe = \infty$), the concentration fronts are two shocks, as indicated by the equilibrium theory. This case constitutes a severe test for the numerical models because of the very sharp transitions caused by the large Peclet number and the self-sharpening behavior. It can be observed that SAG performs very satisfactorily with much less oscillations than QUDS (Figure 2) while CDS produces disastrous oscillatory results (see Figure 3). The exact

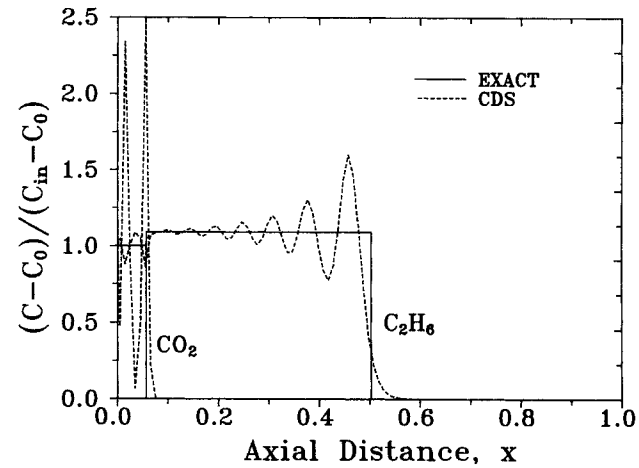

Figure 3. Simulations by the centered scheme CDS for the same case as in Figure 2.

Errors for CDS: $(\|e\|_2, \|e\|_\infty) = (0.1796, 1.4520)$.

Table 3. Numerical Errors for Isothermal Adsorption of CO_2 at $\tau = 3{,}000$

Pe_Δ	SAG		QUDS		CDS		UDS	
	$\|e\|_2$	$\|e\|_\infty$	$\|e\|_2$	$\|e\|_\infty$	$\|e\|_2$	$\|e\|_\infty$	$\|e\|_2$	$\|e\|_\infty$
2,000	0.0614	0.3789	0.1120	0.4061	0.1543	0.5367	0.1858	0.4575
1,000	0.0225	0.2261	0.0670	0.3537	0.1150	0.5001	0.1439	0.4421
500	0.0060	0.0711	0.0559	0.3787	0.0967	0.5012	0.1246	0.4228

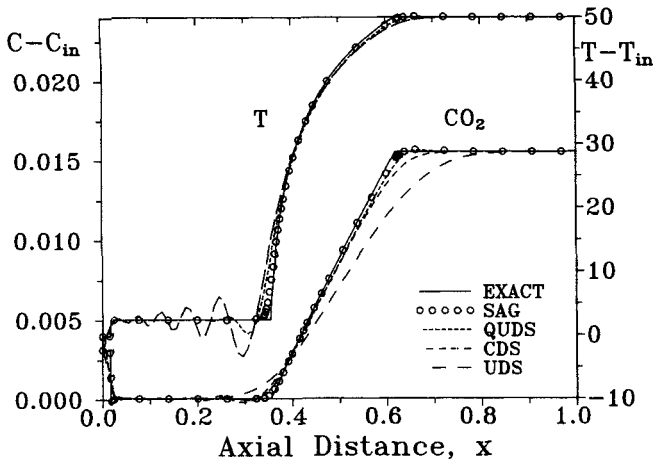

Figure 4. Profiles at $\tau = 2{,}000$ for adiabatic desorption of CO_2 with $Pe_\Delta = 100$.

$(\|e\|_2, \|e\|_\infty) = (0.0030, 0.0733)$ for SAG, (0.0152, 0.0979) for QUDS, (0.0294, 0.1388) for CDS and (0.0663, 0.2282) for UDS.

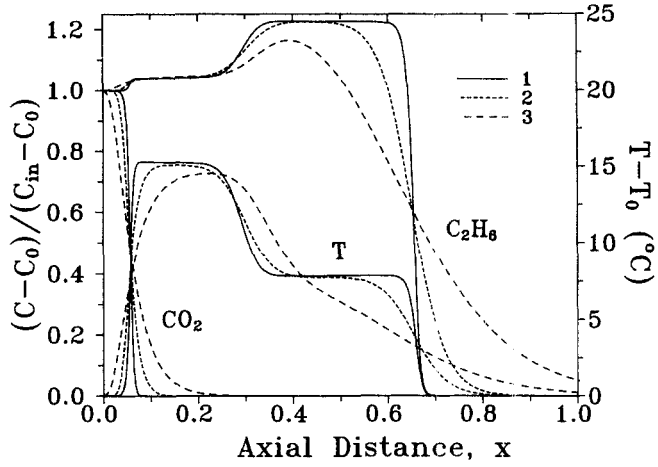

Figure 5. Nonisothermal adsorption of CO_2 and C_2H_6.

1. equilibrium; 2. moderately kinetics-controlled; and 3. strongly kinetics-controlled situations. Simulations by SAG with $Pe_\Delta = 2.5$.

solutions plotted in Figures 2–4 represent the equilibrium theory's solutions.

2. *Elution of a Partially-Saturated Bed by a Cool Dilute Feed (CO_2).* The pressure and temperature variations are $p_0 = 1{,}000$, $p_{in} = 200$ (Pa) and $T_0 = 327.15$, $T_{in} = 277.15$ (K). With $Pe = \infty$, the fronts are composed of a simple wave and a shock (Figure 4). The transitions being less steep, deviations of the numerical models are much less important than in the previous case. Again, SAG is very satisfactory and QUDS produces acceptable results with small oscillations. CDS and UDS are penalized by their large oscillations and false diffusion, respectively.

Simulations in kinetics-controlled situations

For real adsorption systems, resistances to heat and mass transfers constitute dispersing factors and cause concentration and temperature fronts to broaden. Such effects of finite transfer rates are illustrated in Figure 5 in the case of non-isothermal adsorption of the binary mixture CO_2 and C_2H_6. The following initial and feed conditions are chosen: $p_{0,1} = p_{0,2} = 10^{-5}$, $p_{in,1} = 10^3$, $p_{in,2} = 700$ Pa and $T_0 = T_{in} = 297.15$ K. The three cases considered in the figure correspond to: 1. equilibrium case; 2. standard case with the transfers coefficients defined in Table 2; and 3. slow kinetics case with $D_{i1} = 10^{-17}$ and $D_{i2} = 10^{-18}$ m^2/s. The numerical results reported in Figure 5 are obtained by using SAG with a small grid Peclet number ($Pe_\Delta = 2.5$) and will be considered as the exact solutions for subsequent comparisons.

In Table 4 are given errors of the four numerical models with $Pe_\Delta = 10$ for the above-described three cases and at $\tau = 1{,}000$, 5,000. The comparison of the profile curves at $\tau = 1{,}000$ are shown in Figures 6–8. It can be seen that SAG yields in all the cases considerably higher precisions than the uniform schemes, in particular, than CDS and UDS. When transitions are sufficiently broadening (strongly kinetics-controlled case, Figure 8), all the numerical methods give satisfactory simulations, except for UDS: its false diffusion remains important with respect to all the true physical dispersive forces.

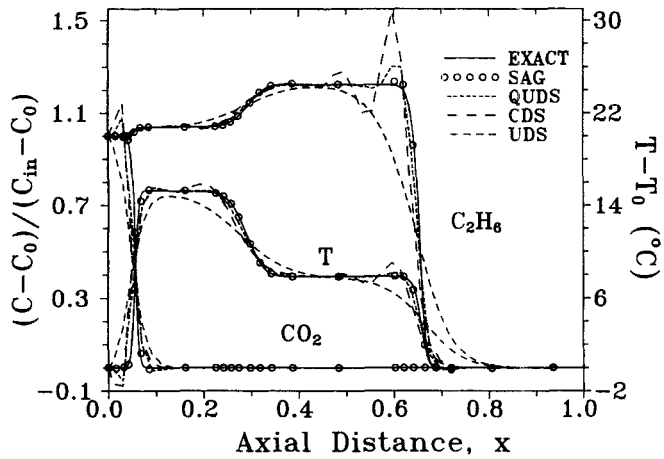

Figure 6. Comparison of profile curves at $\tau = 1{,}000$ in the case of equilibrium adsorption.

Table 4. Numerical Errors for Nonisothermal Adsorption of CO_2 and C_2H_6

Case	Time	SAG		QUDS		CDS		UDS	
	τ	$\|e\|_2$	$\|e\|_\infty$	$\|e\|_2$	$\|e\|_\infty$	$\|e\|_2$	$\|e\|_\infty$	$\|e\|_2$	$\|e\|_\infty$
1	1,000	0.0074	0.0719	0.0342	0.2479	0.0630	0.3977	0.0843	0.3572
	5,000	0.0052	0.0541	0.0499	0.3149	0.0853	0.4472	0.0966	0.5393
2	1,000	0.0037	0.0222	0.0092	0.0737	0.0205	0.1473	0.0545	0.2401
	5,000	0.0012	0.0044	0.0113	0.0659	0.0323	0.2126	0.0656	0.3608
3	1,000	0.0026	0.0103	0.0027	0.0187	0.0077	0.0352	0.0346	0.1361
	5,000	0.0007	0.0015	0.0038	0.0213	0.0091	0.0401	0.0460	0.2080

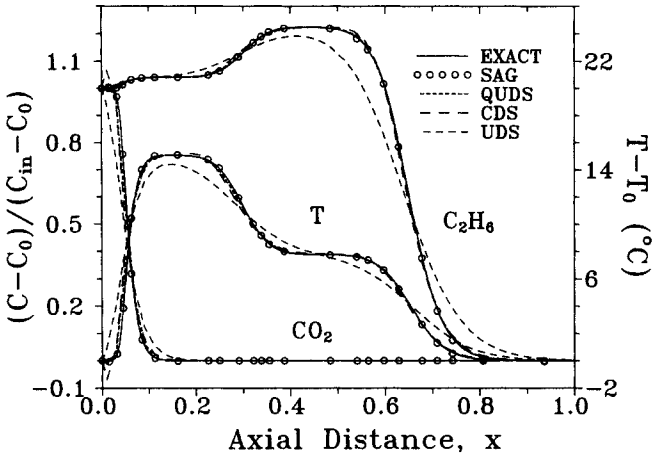

Figure 7. Comparison of profile curves at $\tau = 1{,}000$ for the moderately kinetics-controlled case.

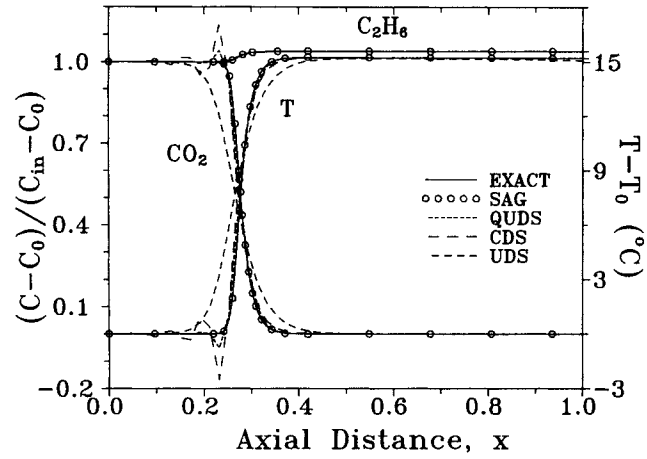

Figure 9. Same as Figure 7 at $\tau = 5{,}000$.

For the moderately kinetics-controlled case (Figure 7), CDS exhibits again oscillations as in the equilibrium case (Figure 6). Finally, the uniform schemes produce more and more perceptible numerical inaccuracies as the fronts travel along the bed (see Table 4). This conclusion is further demonstrated by the comparison between Figures 7 and 9 in which the profiles are plotted at two different times.

Conclusions

A finite difference-based numerical method for solving a general theoretical model has been discussed that describes sorption of a multicomponent system in a fixed bed. The fixed bed is composed of biporous pellets and sorption occurs under nonequilibrium and nonisothermal conditions. The parabolic profile approach was introduced to simplify the numerical treatment of transfers within the pellets. This numerical method applies a simple solution-adaptive gridding technique (SAG) and a quadratic upstream differencing scheme (QUDS) to describe accurately sharp transitions without excessive calculation costs. Moreover, faced with the possible stiffness of particle kinetics equations occurring frequently in kinetics separations, the present method adopts a noniterative implicit solution procedure to avoid any convergence difficulty. Therefore, it can be applied to either near-equilibrium or kinetics-controlled situations.

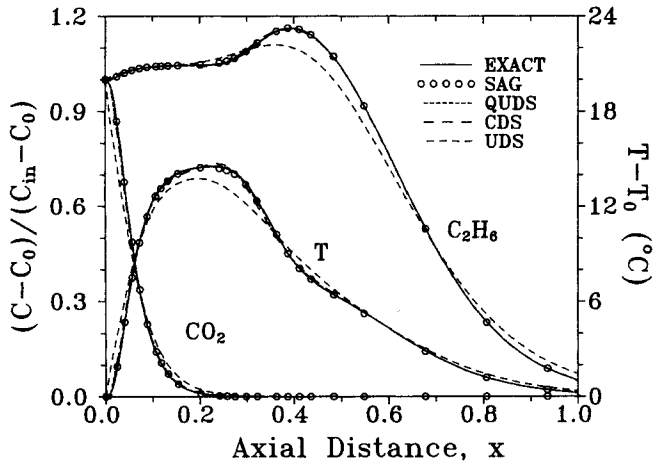

Figure 8. Comparison of profile curves at $\tau = 1{,}000$ for the strongly kinetics-controlled case.

Numerical experiments were undertaken in the case of one-, two- and three-transition systems under both equilibrium and nonequilibrium conditions. It is shown that among the currently-used uniform differencing schemes, the second-order centered and first-order upstream differencing schemes (CDS and UDS) should be used with caution in fixed-bed simulations. The former may suffer from large oscillations while the latter gives important, purely-numerical diffusion. In the case of UDS, numerical diffusion is often so significant that the true physical dispersing effects (axial dispersion and adsorption kinetics) can be highly overestimated. Increasing number of grids to reduce false diffusion is quite inefficient because of the first-order precision of the scheme. It can be expected that similar remarks hold also for bulky separation problems (constant pressure systems) where fronts are generally more self-sharpening.

Improvements have been observed with the use of QUDS which exhibits much less oscillations and false diffusion than CDS and UDS, respectively. Consequently, QUDS is believed to be largely preferable in fixed-bed simulations, though numerical oscillations may occur sometimes.

Finally, the use of SAG considerably improved the present model, making it possible to describe sharp transitions very well with much less computational grids than those used by uniform schemes.

Notation

a_1, a_2 = constants in the definition of the arclength function (Eq. 22)
B = mobility of adsorbates, s
B_c = modified mobility of adsorbates defined by Eq. 1, s
c = gaseous concentration in the bed voids, kg/m^3
c_p = gaseous concentration in the macropores, kg/m^3
C_M = volumetric heat capacity of the gas mixture, J/m^3/K
C_S = volumetric heat capacity of the adsorbent pellets, J/m^3/K
D = axial dispersion coefficient, m^2/s
D_i = microporous diffusion coefficient, m^2/s
D_p = macroporous diffusion coefficient, m^2/s
$\|e\|$ = error norms defined by Eq. 26
E, F = constant parameters defined by Eq. 17

h_p = heat transfer coefficient between the pellets and the mixture, W/m^2/K
h_w = overall heat transfer coefficient at the column wall, W/m^2/K
ΔH = heat of adsorption, J/kg
J = diffusional flux density, kg/m^2/s
k_p = external film mass transfer coefficient, m/s
L_b = bed length, m
m = number of adsorbates
N = number of computational grids
p = adsorbate partial pressure, Pa
Pe = Peclet number ($Pe_k = uL_b/D_k$ for $k \le m$ and $Pe_{m+1} = uL_bC_M/\lambda_M$)
Pe_Δ = grid Peclet number ($= Pe/N$)
q = quantities adsorbed in the crystallites, kg/m^3
Q = derivatives of adsorption isotherms defined by Eq. 16
Q_k^* = constant parameter $= Q_{kk}$ at the reference state
r_i = spherical coordinate at the crystal scale, m
r_p = spherical coordinate at the pellet scale, m
R = gas constant, J/kg/K
R_b = column's radius, m
R_i = radius of crystallites, m
R_p = radius of pellets, m
S = cell arc-length function
S_{lim} = limiting value for the cell arc-length function
t = time, s
T_f = temperature of the gas mixture, K
T_s = temperature of the adsorbents, K
T_w = temperature of the column wall, K
u = interstitial velocity, m/s
U = constant parameter defined by Eq. 17
V = constant parameter defined by Eq. 17, m^{3}K/J
x = dimensionless axial coordinate ($= z/L_b$)
Δx = dimensionless spatial increment
z = axial coordinate, m
Z = parameter defined by Eq. 16

Greek letters

α_H = ratio of time constants defined by Eq. 18
α_I = ratio of time constants defined by Eq. 19
α_P = ratio of time constants defined by Eq. 20
α_W = ratio of time constants defined by Eq. 21
ϵ_b = bed porosity
ϵ_p = pellet porosity
λ_M = effective heat conductivity of the gas mixture, W/m/K
μ = chemical potential, J/kg
τ = dimensionless time ($= ut/L_b$)
$\Delta\tau$ = dimensionless time increment

Subscripts

i = grid i
k = component k
0 = initial values
in = values at the inlet

Superscripts

$\bar{}$ = volume average values
$\bar{\bar{}}$ = quantities averaged over both the crystal and pellet volumes
n = discrete time level

Literature Cited

Blom, J. G., J. M. Sanz-Serna, and J. G. Verwer, "On Simple Moving Grid Methods for One-Dimensional Evolutionary Partial Differential Equations," *J. Comput. Phys.*, **74**, 191 (1988).

Carter, J. W., and H. Husain, "The Simultaneous Adsorption of Carbon Dioxide and Water Vapour by Fixed Beds of Molecular Sieves," *Chem. Eng. Sci.*, **29**, 267 (1974).

Chihara, K., and M. Suzuki, "Simulation of Nonisothermal Pressure Swing Adsorption," *J. Chem. Eng. Japan*, **16**(1), 53 (1983).

Cooney, D. O., "Numerical Investigation of Adiabatic Fixed-Bed Adsorption," *Ind. Eng. Chem. Process Des. Dev.*, **13**(4), 368 (1974).

Doong, S. J., and R. T. Yang, "Bulk Separation of Multicomponent Gas Mixtures by Pressure Swing Adsorption: Pore/Surface Diffusion and Equilibrium Models," *AIChE J.*, **32**(3), 397 (1986).

Dwyer, H. A., "Grid Adaption for Problems in Fluid Dynamics," *AIAA J.*, **22**(12), 1705 (1984).

Hoffman, J. D., "Relationship between the Truncation Errors of Centered Finite-Difference Approximations on Uniform and Nonuniform Meshes," *J. Comput. Phys.*, **46**, 469 (1982).

Hu, S. S., A. K. Didwania, W. G. May, J. C. Pirkle, and W. E. Schiesser, "An Adaptive Grid for the Computer Simulation of Separation Systems," *Proc. IMACS Tenth World Cong.*, Montreal (1982).

Hu, S. S., and W. E. Schiesser, "An Adaptive Grid Method in the Numerical Method of Lines," *Proc. Fourth IMACS Int. Symp. on Computer Methods for PDEs*, R. Vichnevetsky and R. S. Stepleman, eds., Rutgers University (1981).

Huang, C. C., and J. R. Fair, "Study of the Adsorption and Desorption of Multiple Adsorbates in a Fixed Bed," *AIChE J.*, **34**(11), 1861 (1988).

Leonard, B. P., "A Stable and Accurate Convective Modelling Procedure Based on Quadratic Upstream Interpolation," *Comput. Methods Appl. Mech. Eng.*, **19**, 59 (1979).

Liapis, A. I., and O. K. Crosser, "Comparison of Model Predictions with Nonisothermal Sorption Data for Ethane-Carbon Dioxide Mixtures in Beds of 5A Molecular Sieves," *Chem. Eng. Sci.*, **37**(6), 958 (1982).

Patel, M. K., N. C. Markatos, and M. Cross, "A Critical Evaluation of Seven Discretization Schemes for Convection-Diffusion Equations," *Int. J. Numer. Methods Fluids*, **5**, 225 (1985).

Peyret, R., and T. D. Taylor, *Computational Methods for Fluid Flow*, Springer-Verlag, New York (1983).

Raghavan, N. S., and D. M. Ruthven, "Numerical Simulation of a Fixed-Bed Adsorption Column by the Method of Orthogonal Collocation," *AIChE J.*, **29**(6), 922 (1983).

Rhee, H. K., and N. R. Amundson, "An Analysis of an Adiabatic Column: Part I. Theoretical Development," *Chem. Eng. J.*, **1**, 241 (1970).

Rhee, H. K., E. D. Heerdt, and N. R. Amundson, "An Analysis of an Adiabatic Column: II. Adiabatic Adsorption of a Single Solute," *Chem. Eng. J.*, **1**, 279 (1970).

Ruthven, D. M., *Principles of Adsorption and Adsorption Processes*, Wiley Interscience, New York (1984).

Sanz-Serna, J. M., and I. Christie, "A Simple Adaptive Technique for Nonlinear Wave Problems," *J. Comput. Phys.*, **67**, 348 (1986).

Sod, G. A., "A Survey of Several Difference Methods for Systems of Nonlinear Hyperbolic Conservation Laws," *J. Comput. Phys.*, **27**, 1 (1978).

Thompson, J. F., "Grid Generation Techniques in Computational Fluid Dynamics," *AIAA J.*, **22**(11), 1505 (1984).

White, A. B., "On the Numerical Solution of Initial/Boundary-Value Problems in One Space Dimension," *SIAM J. Numer. Anal.*, **19**(4), 683 (1982).

Yang, R. T., *Gas Separation by Adsorption Process*, Butterworths, Boston (1987).

Appendix

Equations 11-15 generally are coupled strongly through adsorption isotherms and transfer coefficients. Usually, these equations are solved by an iterative manner: the column equations (Eqs. 11-12) and the particle equations (Eqs. 13-15) are first decoupled, and an iterative procedure is then carried out. The main drawback of these methods lies in the possible limitation on time steps by the convergence consideration, especially when the kinetics equations are stiff. To have a generally-applicable technique, we will use an implicit solution procedure.

After discretization in time and space, Eqs. 14 and 15 become:

$$\sum_{j=1}^{m+1} Q_{kj}\omega_j^{n+1/2} + (0.5\alpha_{Ik}Q_k^*\Delta\tau)\omega_k^{n+1/2} = \sum_{j=1}^{m+1} Q_{kj}\omega_j^n + (0.5\alpha_{Ik}Q_k^*\phi_k\Delta\tau)\bar{c}_{pk}^{n+1/2}$$

$$-V\sum_{j=1}^{m+1} Z_j\omega_j^{n+1/2} + (1+0.5\alpha_H\Delta\tau)\omega_{m+1}^{n+1/2} = -V\sum_{j=1}^{m+1} Z_j\omega_j^n + \omega_{m+1}^n + (0.5\alpha_H\Delta\tau)T_f^{n+1/2}$$

Divide above equations by their diagonal elements of the left hand side:

$$\sum_{j=1}^{m+1}[\delta_{kj}+(1-\delta_{kj})a_{kj}]\omega_j^{n+1/2} = \begin{cases} b_k + d_k\bar{c}_{pk}^{n+1/2} & k\le m \\ b_k + d_kT_f^{n+1/2} & k=m+1 \end{cases}$$

where δ_{kj} is the Kronecker delta, and for $k\le m$:

$$a_{kj} = \frac{Q_{kj}}{Q_{kk}+0.5\alpha_{Ik}Q_k^*\Delta\tau} \qquad b_k = \sum_{j=1}^{m+1} a_{kj}\omega_j^n$$

$$d_k = \frac{0.5\alpha_{Ik}Q_k^*\phi_k\Delta\tau}{Q_{kk}+0.5\alpha_{Ik}Q_k^*\Delta\tau}$$

For $k=m+1$:

$$a_{kj} = -\frac{VZ_j}{g} \qquad b_k = \frac{\omega_k^n}{g} + \sum_{j=1}^{m+1} a_{kj}\omega_j^n$$

$$d_k = \frac{\alpha_H\Delta\tau}{2g} \qquad (g = 1+0.5\alpha_H\Delta\tau - VZ_k)$$

The above equation gives the expression of ω as functions of $\bar{c}_p$ and T_f:

$$\omega_k^{n+1/2} = f_k + \sum_{j=1}^{m} g_{kj}\bar{c}_{pj}^{n+1/2} + g_{km+1}T_f^{n+1/2} \qquad \text{(A1)}$$

with

$$f_k = \sum_{j=1}^{m+1} A_{kj}b_j \qquad g_{kj} = A_{kj}d_j \quad \text{for } k,j = 1,2,\ldots,m+1$$

The matrix A is defined by:

$$A = \begin{pmatrix} 1 & a_{12} & \cdots & a_{1\,m+1} \\ a_{21} & 1 & \cdots & a_{2\,m+1} \\ \vdots & \vdots & \cdots & \vdots \\ a_{m+1\,1} & a_{m+1\,2} & \cdots & 1 \end{pmatrix}^{-1}$$

Under the equilibrium condition ($\alpha_I = \alpha_H = \infty$), the matrix A becomes a unit matrix.

Introduction of Eq. A1 into the discretized Eq. 13 yields:

$$\sum_{j=1}^{m}[\delta_{kj}+(1-\delta_{kj})r_{kj}]\bar{c}_{pj}^{n+1/2} = \alpha_k + \beta_k c_k^{n+1/2} + \gamma_k T_f^{n+1/2} \qquad k = 1,2,\ldots,m$$

with

$$h_{kj} = \sum_{i=1}^{m+1} Q_{ki}g_{ij} \qquad e = 1+0.5\alpha_{Pk}\Delta\tau + Fh_{kk} \qquad r_{kj} = \frac{Fh_{kj}}{e}$$

$$\alpha_k = \frac{1}{e}\left[c_{pk}^n + F\sum_{j=1}^{m+1} Q_{kj}(\omega_j^n - f_j)\right]$$

$$\beta_k = \frac{\alpha_{Pk}\Delta\tau}{2e} \qquad \gamma_k = -\frac{F}{e}\sum_{j=1}^{m+1} Q_{kj}g_{jm+1}$$

Undertaking similar algebraic operations, we obtain a relation between the averaged macroporous concentration $\bar{c}_p$ and the column variables c_k, T_f:

$$\bar{c}_{pk}^{n+1/2} = u_k + \sum_{j=1}^{m} v_{kj}\,c_j^{n+1/2} + v_{km+1}T_f^{n+1/2} \qquad \text{(A2)}$$

where

$$u_k = \sum_{j=1}^{m} B_{kj}\alpha_j \qquad v_{kj} = B_{kj}\beta_j \quad (k\le m) \quad \text{and} \quad v_{km+1} = \sum_{j=1}^{m} B_{kj}\gamma_j$$

B_{kj} are elements of the following $(m\times m)$ matrix:

$$B = \begin{pmatrix} 1 & r_{12} & \cdots & r_{1m} \\ r_{21} & 1 & \cdots & r_{2m} \\ \vdots & \vdots & \cdots & \vdots \\ r_{m1} & r_{m2} & \cdots & 1 \end{pmatrix}^{-1}$$

Again the above matrix becomes a unit matrix under the equilibrium condition ($\alpha_P = \infty$).

Now, the particle variables in the column equations (Eqs. 11 and 12) can be replaced by Eqs. A1 and A2 and the following set of equations is obtained with c_k as the only unknowns:

$$a_i^{(k)}\,c_{k,i-2} + b_i^{(k)}\,c_{k,i-1} + \sum_{j=1}^{m+1} d_i^{(k,j)}\,c_{j,i} + e_i^{(k)}c_{k,i+1} = f_i^{(k)} \qquad \text{(A3)}$$

$k = 1,2,\ldots,m+1 \quad i = 1,2,\ldots,N$ with $a_1^{(k)} = b_1^{(k)} = a_2^{(k)} = e_N^{(k)} = 0$

The superscript $n+1/2$ was dropped for reading clarity and $c_{m+1} = T_f$. If the column variables c_k are known by the solution of the above system, the particle variables can be readily determined by a back substitution through Eqs. A2 and A1.

The system (Eq. A3) can be solved by an iterative method in which only the equation of a single component is considered at each step. The recurrence formulation at the lth iteration is given by:

$$a_i^{(k)}\, c_{k,i-2}^{(l)} + b_i^{(k)}\, c_{k,i-1}^{(l)} + d_i^{(k,k)}\, c_{k,i}^{(l)} + e_i^{(k)}\, c_{k,i+1}^{(l)} = f_i^{(k)} - \sum_{j=1}^{k-1} d_i^{(k,j)}\, c_{j,i}^{(l)} - \sum_{j=k+1}^{m+1} d_i^{(k,j)}\, c_{j,i}^{(l-1)}$$

The above equation consititutes a quadrdiagonal matrix which can be solved by an algorithm of Thomas-type taking into account the asymmetry. This procedure is iterated until the following criterion is satisfied:

$$\| [c_{k,i}^{(l)} - c_{k,i}^{(l-1)}] / c_{k,i}^{(l)} \|_1 \leq \epsilon \quad k = 1,2,\ldots,m+1,2,\ldots,N$$

In this work, $\epsilon = 10^{-6}$ is used for all the simulations.

The above iterative method was compared to a direct Gaussian elimination method in which the unknown variables are first arranged by components and then by grids to have a band matrix. The resulting vector of the dependent variables has a dimension $(m+1)N$ and is related to the original unknown variables $c_{k,i}$ by the following equation:

$$X[k + (m+1)(i-1)] = c_{k,i}$$
$$k = 1,2,\ldots,m+1 \text{ and } i = 1,2,\ldots,N$$

This special arrangement converts the system of Eq. A3 into a band system of band width $6(m+1)-1$ with only $m+4$ nonzero diagonal elements. Its solution was obtained by a suitable algorithm for general band systems which considers the particular structure of the present system. The iterative method described previously proved faster than this direct method and therefore was applied in the simulations.

In the above-developed solution procedure, inversion of two matrice of dimensions $(m+1)\times(m+1)$ and $m \times m$ is required for each grid. This may increase calculation times considerably compared to equilibrium models. As the major advantage, the present method does not have any stability and convergence problems and may allow larger time steps.

Manuscript received May 30, 1990, and revision recieved Dec. 21, 1990.